JOURNAL OF Materials CHEMISTRY

Hybrid macroporous materials for heavy metal ion adsorption†

Rick C. Schroden,[a] Mohammed Al-Daous,[a] Sergey Sokolov,[a] Brian J. Melde,[a] Justin C. Lytle,[a] Andreas Stein,*[a] Mari Carmen Carbajo,[b] José Torralvo Fernández[b] and Eduardo Enciso Rodríguez[b]

[a]*University of Minnesota, Department of Chemistry, Minneapolis, MN 55455, USA. E-mail: stein@chem.umn.edu*
[b]*Universidad Complutense de Madrid, Facultad de Ciencias Químicas, 28040 Madrid, Spain*

Received 26th April 2002, Accepted 9th July 2002
First published as an Advance Article on the web 3rd October 2002

Hybrid macroporous materials with thiol functional groups attached to titania and zirconia frameworks have been prepared *via* colloidal crystal templating techniques for use as heavy metal ion adsorbents. Synthesis procedures are described for the preparation of thiol–metal oxide materials containing either siloxane or sulfonate linkages. The hybrid macroporous materials were characterized by SEM, FT-IR, ^{29}Si MAS NMR, elemental analysis, and nitrogen adsorption. The materials contained high levels of chemically anchored thiol groups and had uniform porous structures. The hybrid macroporous materials were effective adsorbents for the removal of heavy metal ions from solution, with adsorption capacities ranging from 0.33 to 1.41 mmol g^{-1} for mercury(II) ions and 0.27 to 1.24 mmol g^{-1} for lead(II) ions. The hybrid materials remained effective for metal ion adsorption after regeneration by an acid wash, with metal ion loading capacities of the recycled materials being on average two-thirds that of the original capacities. The metal ion adsorption capacity and reusability of hybrid macroporous materials makes them promising adsorbents for wastewater cleanup.

Introduction

Heavy metal ions, especially mercury and lead, are highly toxic environmental pollutants. The development of techniques for removal of these metal ions from waste streams has, therefore, been a very active area of research. Effective approaches to the removal of heavy metal ions from solution have involved the use of various solid adsorbents, including activated carbon,[1] organic ion exchange polymers,[1] and numerous thiol-functionalized silica-based supports, including silica gel,[2,3] clays,[4] and mesoporous silica.[5–14] With these adsorbents, the organic functionalities typically serve to form complexes with heavy metal ions through acid–base reactions, and the solid support allows easy removal of the loaded adsorbent from the liquid waste. The thiol–silica adsorbents have typically been prepared by either the covalent grafting of thiol–alkoxysilanes to the silica supports *via* reaction of the alkoxy groups with the surface hydroxyl groups,[4,6–8,10,11] or by direct synthesis co-condensation of thiol–alkoxysilanes with silica precursors in the presence of organic templates or structure directing molecules.[9,12–15]

A commonly used approach for the preparation of heavy metal ion adsorbents has involved the use of surfactant micelles to template hybrid mesoporous structures.[6–15] This approach followed the introduction of ordered mesoporous materials prepared by micellar templating a decade ago.[16–19] Materials prepared by this technique typically have pore sizes ranging from 2–10 nm. More recently a different approach, utilizing polymer colloidal crystals as templates, has allowed the preparation of macroporous materials with typical pore sizes of 100 nm–1 μm. Variations of the colloidal crystal templating approach have allowed the preparation of three-dimensionally ordered macroporous (3DOM) materials with diverse compositions,[20] including metal oxides,[21–23] metals,[24–26] semiconductors,[27–29] polymers,[30,31] carbon,[32] and hybrid materials.[33–35] While the specific surface area of macroporous materials is typically lower than that of mesoporous materials, the large pores in these materials have been found to improve the accessibility of reactants to the active sites of the material.[36,37] The synthetic flexibility of the colloidal crystal templating approach is also beneficial for tailoring the reactivity of porous materials. Organic functionalization of porous materials provides a means of tuning the surface properties to control host/guest interactions and the hydrophobicity or hydrophilicity of the surface. Functionalization also allows control over the bulk properties of the materials, including the mechanical and optical properties, as well as tailoring the refractive index of the material for photonic applications.

In the current report, colloidal crystal templating techniques were used to prepare hybrid macroporous materials for heavy metal ion adsorption. Hybrid macroporous materials constructed of both titania and zirconia supports, functionalized with thiol groups, were synthesized. Hybrid macroporous materials have previously been prepared, however the compositions have been limited to silica materials. The functional groups that have been chemically attached to macroporous silica include vinyl,[33] organically-modified polyoxometalate clusters,[34,35] and organic dyes.[38] The benefit of utilizing titania and zirconia as support materials is that they offer multiple modes of functionalization, including siloxane (M–O–Si),[39] sulfonate (M–O–S),[40] and phosphonate (M–O–P)[41–43] linkages. Two of these bonding modes, siloxane and sulfonate linkages, were studied here since precursors containing these linking groups and thiol functionalities are commercially available. The porous adsorbents were prepared *via* direct synthesis procedures, which allowed the incorporation of high levels of thiol functionalities into the materials. Thiol-functionalized titania and zirconia with siloxane linkages could both be prepared *via* single-step templating procedures. However, the procedures for the incorporation of thiol–sulfonate groups into the macroporous materials varied for the two metal oxide compositions. The higher moisture sensitivity of zirconium

†Basis of a presentation given at Materials Discussion No. 5, 22–25 September 2002, Madrid, Spain.
Electronic supplementary information (ESI) available: IR spectra of samples **T1**, **Z1**, **T2** and **Z2** and ^{1}H–^{29}Si CP MAS NMR spectra of samples **T1** and **Z1**. See http://www.rsc.org/suppdata/jm/b2/b204065b/

alkoxides necessitated the use of a two-step templating procedure for the preparation of thiol–zirconia with sulfonate linkages, whereas a single-step procedure was used for the preparation of thiol–titania with the same linking groups.

In this report, the procedures used to prepare the hybrid porous materials, as well as their structures and compositions, are described and compared. Results of the capacity of the hybrid macroporous materials to adsorb mercury and lead ions from aqueous solution are provided. It was found that all of the hybrid macroporous materials exhibited an affinity for heavy metal ions. Washing the loaded materials with an acid removed the heavy metal ions, allowing the materials to be reused. Subsequent tests of the metal ion adsorption capacity demonstrated that the regenerated materials remained effective for removal of metal ions from solution.

Experimental

Materials

Reagents were obtained from the following sources: (3-mercaptopropyl)trimethoxysilane (MPTMS), 2-mercaptoethanesulfonic acid (sodium salt) (MESA), 3-mercapto-1-propanesulfonic acid (sodium salt) (MPSA), titanium(IV) propoxide, zirconium(IV) propoxide (70 wt.% solution in *n*-propanol), zirconyl chloride octahydrate, HCl (37%), *n*-propanol, tetrahydrofuran (THF), methyl methacrylate (MMA), and 2,2′-azobis(2-methylpropionamidine) dihydrochloride, were from Aldrich; mercury(II) chloride and lead(II) nitrate were from Mallinckrodt; absolute ethanol was from Aaper Alcohol and Chemical Co.; acetone was from Pharmco Products Inc. All chemicals were used as received without further purification. Water used in all syntheses was distilled and deionized to 17.7 MΩ cm.

Synthesis of PMMA colloidal crystal templates

Monodisperse poly(methyl methacrylate) (PMMA) spheres were synthesized using an optimized version of literature techniques[44,45] and packed into colloidal crystals. PMMA spheres were synthesized at 70–80 °C from mixtures of typical composition: 1.4–1.65 L of water, 250–600 mL of MMA, and 1.5 g 2,2′-azobis(2-methylpropionamidine) dihydrochloride as an azo initiator. Water and MMA were added to a five-neck round-bottom flask, to which was attached an electric stirrer driving a glass stirring shaft with a Teflon stirrer blade, a water-cooled condenser, a pipet connected to a house supply of nitrogen gas, and a thermocouple probe attached to a temperature controller. The mixture was stirred at approximately 350 rpm, while being heated to 70–80 °C and purged with nitrogen. After stabilization of the temperature at an elevated level, the azo initiator was added and the reaction was allowed to proceed for 1–2 h, producing colloidal PMMA spheres. The colloidal polymer was filtered through glass wool to remove any large agglomerates. PMMA colloidal crystals were formed by centrifuging the colloid at 1500 rpm for 24 h, decanting the water, and allowing the solid to dry for 3 days. Before being used as templates, the PMMA colloidal crystal pellets were crushed with a metal spatula to form a powder. PMMA spheres used in the syntheses of macroporous materials had diameters of 300 ± 5 nm and 480 ± 5 nm, as measured by SEM.

Synthesis of hybrid porous materials

Macroporous thiol-functionalized titania and zirconia materials with propyl–siloxane, ethyl–sulfonate, and propyl–sulfonate linkages were prepared by PMMA colloidal crystal templating with subsequent removal of the organic template by solvent extraction. The designations below refer only to the type of support (titania or zirconia) and functional group, and are not meant to represent the stoichiometric chemical formulas.

T1, (TiO_2-O_3Si-Pr-SH). 3DOM thiol–titania materials with propyl–siloxane linkages were prepared from precursor solutions of typical composition: 8 mL of ethanol, 1 mL of HCl, 6 mL of titanium(IV) propoxide, 1 mL of water, 2 mL of MPTMS. The reagents were added to a small vial containing a magnetic stir bar in the order listed above. A clear solution formed after each step. The precursor solution was stirred at room temperature for several minutes. Dried PMMA sphere colloidal crystals were crushed to a powder and deposited in millimeter-thick layers on filter paper in a Büchner funnel. With suction applied to the Büchner funnel, the precursor solution was applied dropwise to completely wet the PMMA powder. Equal amounts of PMMA and precursor solution, by mass, were used. The composite sample was allowed to dry in air at room temperature for 24 h, followed by drying at 80 °C for 10 h. The PMMA template was removed from the sample by extraction for 5 days in a refluxing solution of 1 : 1 (v/v) THF and acetone. The powder product was recovered by filtration and washed with THF, then acetone.

EA (wt.%): Ti (27.97), S (7.18), C (13.60). Carbon content from thiol functional group and polymer template, assuming no residual solvent (calculated from S and C analysis): $C_{functional}$ (8.07), C_{PMMA} (5.53). FTIR (Si–O bands, cm^{-1}): 1141, 1040. SEM: pore size 265 ± 5 nm, template size 300 ± 5 nm. BET surface area: 37 m^2 g^{-1}. ^1H–^{29}Si CP MAS NMR, ppm: −68 (T^3), −58 (T^2).

T2, (TiO_2-O_3S-Et-SH). 3DOM thiol–titania materials with ethyl–sulfonate linkages were prepared from precursor solutions of typical composition: 5 mL of water, 1.19 g of MESA, 1.5 mL of HCl, 8 mL of ethanol, and 6 mL of titanium(IV) propoxide. The reagents were added to a small vial containing a magnetic stir bar in the order listed above. The alkoxide was added very slowly dropwise. With each drop of alkoxide added to the precursor solution a precipitate formed, but dissolved upon stirring the sample to form a clear solution. The precursor solution was stirred and applied to the PMMA template, followed by sample drying and extraction as described above.

EA (wt.%): Ti (27.92), S (11.40), C (6.54). Carbon content from thiol functional group and polymer template (calculated from S and C analysis): $C_{functional}$ (4.27), C_{PMMA} (2.27). FTIR (S–O bands, cm^{-1}): 1232, 1155, 1047. SEM: pore size 270 ± 5 nm, template size 300 ± 5 nm. BET surface area: 12 m^2 g^{-1}.

T3, (TiO_2-O_3S-Pr-SH). 3DOM thiol–titania materials with propyl–sulfonate linkages were prepared from precursor solutions of typical composition: 5 mL of water, 1.30 g of MPSA, 1.5 mL of HCl, 8 mL of ethanol, and 6 mL of titanium(IV) propoxide. The reagents were added to a small vial containing a magnetic stir bar in the order listed above. The alkoxide was added very slowly dropwise. With each drop of alkoxide added to the precursor solution a precipitate formed, but dissolved upon stirring the sample to form a clear solution. The precursor solution was stirred and applied to the PMMA template, followed by sample drying and extraction as described above.

EA (wt.%): Ti (29.79), S (10.99), C (8.89). Carbon content from thiol functional group and polymer template (calculated from S and C analysis): $C_{functional}$ (6.17), C_{PMMA} (2.72). FTIR (S–O bands, cm^{-1}): 1223, 1149, 1047. SEM: pore size 275 ± 5 nm, template size 300 ± 5 nm. BET surface area: 12 m^2 g^{-1}.

Z1, (ZrO_2-O_3Si-Pr-SH). 3DOM thiol–zirconia materials with propyl–siloxane linkages were prepared from precursor solutions of typical composition: 8 mL of *n*-propanol, 5 mL of zirconium(IV) propoxide, and 1 mL of MPTMS. The reagents were added to a small vial containing a magnetic stir bar in the

order listed above, forming a clear, dark green solution. The precursor solution was stirred and applied to the PMMA template, followed by sample drying and extraction as described above.

EA (wt.%): Zr (43.08), S (4.44), C (12.09). Carbon content from thiol functional group and polymer template (calculated from S and C analysis): $C_{functional}$ (4.99), C_{PMMA} (7.10). FTIR (Si–O bands, cm^{-1}): 1125, 1037. SEM: pore size 415 $\pm$ 5 nm, template size 480 $\pm$ 5 nm. BET surface area: 18 m^2 g^{-1}. ^1H–^{29}Si CP MAS NMR, ppm: −67 (T^3), −57 (T^2).

Z2, (ZrO_2-O_3S-Et-SH). 3DOM thiol–zirconia materials with ethyl–sulfonate linkages were prepared by a two-step templating procedure. First, a precursor solution of composition: 10 mL of water, 10 mL of methanol, 2.0 g of MESA, and 7.0 g zirconyl chloride was prepared. The precursor solution was applied to 10 g of the powdered PMMA template on filter paper in a Büchner funnel, with suction applied. The composite sample was allowed to dry in air for 1 h. A second solution was then prepared with composition: 10 mL of *n*-propanol and 4 mL of zirconium(IV) propoxide. This solution was then applied to the composite sample on a filter paper in a Büchner funnel with suction applied, followed by sample drying and extraction as described above.

EA (wt.%): Zr (41.57), S (8.30), C (8.16). Carbon content from thiol functional group and polymer template (calculated from S and C analysis): $C_{functional}$ (3.11), C_{PMMA} (5.05). FTIR (S–O bands, cm^{-1}): 1243, 1151, 1047. SEM: pore size 450 $\pm$ 5 nm, template size 480 $\pm$ 5 nm. BET surface area: 20 m^2 g^{-1}.

Z3, (ZrO_2-O_3S-Pr-SH). 3DOM thiol–zirconia materials with propyl–sulfonate linkages were prepared by a two-step templating procedure. First, a precursor solution of composition: 10 mL of water, 10 mL of methanol, 2.0 g of MPSA, and 7.0 g zirconyl chloride was prepared. The precursor solution was applied to 10 g of the powdered PMMA template on filter paper in a Büchner funnel, with suction applied. The composite sample was allowed to dry in air for 1 h. A second solution was then prepared with composition: 10 mL of *n*-propanol and 4 mL of zirconium(IV) propoxide. This solution was then applied to the composite sample on a filter paper in a Büchner funnel with suction applied, followed by sample drying and extraction as described above.

EA (wt.%): Zr (45.04), S (8.64), C (8.48). Carbon content from thiol functional group and polymer template (calculated from S and C analysis): $C_{functional}$ (4.85), C_{PMMA} (3.63). FTIR (S–O bands, cm^{-1}): 1241, 1147, 1044. SEM: pore size 460 $\pm$ 5 nm, template size 480 $\pm$ 5 nm. BET surface area: 14 m^2 g^{-1}.

MPTMS gel

A dry gel of the thiol–siloxane precursor, MPTMS, was prepared for the purpose of comparing the IR absorptions of this material with those of the MPTMS-modified metal oxides. 2 mL of MPTMS was mixed with 1 mL of water and 0.5 mL of HCl. The solution was allowed to sit in an open container for several weeks to solidify. The solid product was heated at 80 °C for 10 h, producing a dry, white powder. FTIR (Si–O bands, cm^{-1}): 1119 and 1039.

Metal ion adsorption tests

Heavy metal ion adsorption tests of the hybrid macroporous materials were performed in batch mode. The adsorbents were stirred in aqueous solutions (100 mL) of metal salts for 12 h, using an equal amount by mass (50 mg) of the adsorbent and metal salt, $HgCl_2$ or $Pb(NO_3)_2$. The samples were then washed repeatedly in deionized water, collected by filtration, and allowed to dry prior to elemental analysis. Average loading capacities of duplicate tests are reported. Loading capacities for duplicate tests on the same samples varied within 5%.

Regeneration of adsorbents

After loading the adsorbents with Hg(II) ions as described above, the heavy metal ions were removed from the samples according to literature techniques[4,6,8,9,11] by stirring in 1 M HCl for 8 h. The metal adsorption test was then repeated on the leached adsorbents by the method described above to test the reusability of the materials.

Characterization

Elemental analyses were performed for Ti, Zr, Hg, and Pb at the Department of Geology, University of Minnesota, Minneapolis, MN, and for C and S at Atlantic Microlab Inc., Norcross, GA. Infrared spectroscopy was performed on a Nicolet Magna-IR 760 spectrometer with mid-IR and far-IR capability. Spectra were obtained using the powdered samples in FTIR grade KBr pellets. Scanning electron micrographs (SEM) were obtained on a Hitachi S-800 scanning electron microscope operating at 4 kV. Samples for SEM were dusted on an adhesive conductive carbon disk attached to an aluminium mount and were coated with 70 Å Pt prior to examination. Polymer sphere diameters and macropore sizes were determined from SEM. BET surface areas were measured by nitrogen adsorption using an Advanced Scientific Designs RXM-100 catalyst characterization instrument. Solid-state NMR spectra were obtained on a Chemagnetics CMX-400 Infinity spectrometer at room temperature with a 5 mm zirconia rotor spinning at 5.5 kHz. ^1H–^{29}Si CP MAS NMR spectra (79.49 MHz, 6.5 μs ^1H 90 ° pulse width, 4 s pulse delay) used a PDMS (plasma desorption mass spectroscopy) standard.

Results and discussion

Adsorbent synthesis and characterization

The preparation of macroporous thiol–titania and thiol–zirconia materials *via* direct synthesis routes required careful control of the reaction conditions to prevent premature condensation of the sol–gel precursors and the formation of bulk materials. The best results for the syntheses of macroporous thiol–titania materials were obtained when titanium(IV) propoxide was used as the titania precursor. Titanium alkoxides are very reactive and moisture sensitive, undergoing rapid condensation when exposed to moisture. However, the addition of hydrochloric acid to titanium(IV) propoxide greatly decreases the rate of condensation, allowing the addition of water to the precursor solution without the formation of a precipitate. This was especially important for the preparation of precursor solutions for the thiol–titania materials with sulfonate linkages, since water was required to dissolve the sodium salts of the thiol–sulfonates. Titanium(IV) propoxide is also very viscous, so the precursor solutions were diluted with ethanol to increase penetration through the polymer template.

The order of addition of reagents to the precursor solutions was found to be very important for the preparation of clear precursor solutions. Most orders of addition of the same reagents, other than those given in the Experimental section, resulted in the rapid condensation of solids from the solutions. Since precursor solutions containing both the thiol functional group and the titania precursor could be prepared for all three compositions, single-step templating procedures were used to prepare all of the macroporous thiol–titania materials. The reaction scheme for the preparation of thiol–titania materials with propyl–sulfonate linkages is given in Fig. 1. The procedures used for the preparation of the other two thiol–titania derivatives were similar. Following the colloidal crystal templating step in this procedure, the samples were first dried at

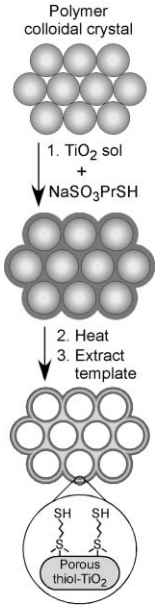

Fig. 1 Reaction scheme for the preparation of macroporous thiol–titania materials containing propyl–sulfonate linkages. The precursors are added to the PMMA colloidal crystal template in a single step, followed by drying at an elevated temperature, and extraction of the template by stirring the sample in a refluxing THF/acetone solution.

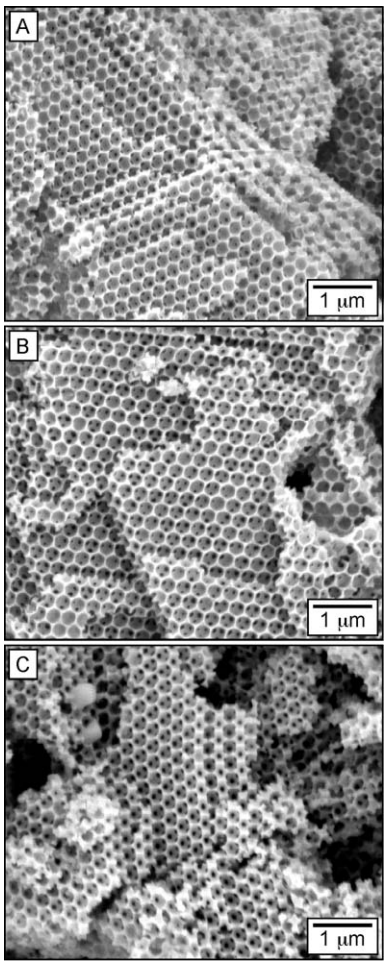

Fig. 2 SEM images of the macroporous thiol–titania materials. (A) **T1**, thiol–titania with propyl–siloxane linkages. (B) **T2**, thiol–titania with ethyl–sulfonate linkages. (C) **T3**, thiol–titania with propyl–sulfonate linkages.

elevated temperatures, and were then stirred in a refluxing THF/acetone solution to extract the PMMA template. This solvent extraction method for template removal was required for these hybrid materials in order to preserve the organic functional groups. The extraction process removed over 99% of the PMMA template, by mass, and the porous thiol–titania products (Fig. 2) contained an average of 6 wt.% PMMA. All of the products had a three-dimensional arrangement of interconnected macropores. The linear shrinkage of the macropores, compared to the diameter of the polymer template, ranged from 8–12%.

The procedures for the preparation of the macroporous thiol–zirconia materials were different than those for the analogous titania samples, because zirconium alkoxides are even more reactive and water sensitive than those of titanium. As a result, neither acid nor water could be added to the zirconium alkoxide precursor without rapid condensation of zirconia. Macroporous thiol–zirconia materials with siloxane linkages could, however, be prepared by a single-step templating procedure since water was not a required precursor. Since zirconium(IV) propoxide is very viscous, it was necessary to dilute it with *n*-propanol to increase penetration through the polymer template. It is noteworthy that the precursor solution for this material, containing zirconium(IV) propoxide, MPTMS, and *n*-propanol, was a clear, dark green solution. The green color is believed to be due to some type of charge-transfer interaction occurring in the precursor solution.

The preparation of the macroporous thiol–zirconia materials with sulfonate linkages required the use of a two-step templating procedure. This procedure is given in Fig. 3 for the preparation of thiol–zirconia materials with propyl–sulfonate linkages. In the first templating step, a solution of zirconyl chloride and the thiol–sulfonate salt was applied to the PMMA template. A zirconium(IV) propoxide solution in *n*-propanol was then added in the second step. Following the colloidal crystal templating steps, the samples were dried and the template was removed by extraction. Similar to the thiol–titania

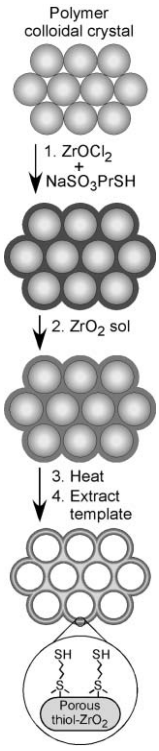

Fig. 3 Reaction scheme for the preparation of macroporous thiol–zirconia materials containing propyl–sulfonate linkages. The precursors are added to the PMMA colloidal crystal template in two steps, followed by drying at an elevated temperature, and extraction of the template by stirring the sample in a refluxing THF/acetone solution.

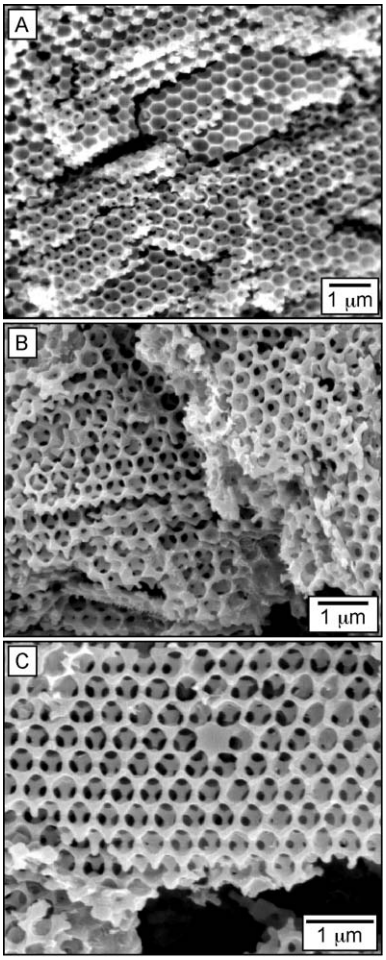

Fig. 4 SEM images of the macroporous thiol–zirconia materials. (A) **Z1**, thiol–zirconia with propyl–siloxane linkages. (B) **Z2**, thiol–zirconia with ethyl–sulfonate linkages. (C) **Z3**, thiol–zirconia with propyl–sulfonate linkages.

preparations, the extraction process removed approximately 99% of the PMMA template from the thiol–zirconia materials, and the products (Fig. 4) contained an average of 9 wt.% PMMA. All of the thiol–zirconia samples exhibited a three-dimensional arrangement of interconnected macropores, however the order of the structures was generally inferior to that of the titania samples. The linear shrinkage of the macropores, compared to the diameter of the polymer template, ranged from 4–14%.

High levels of thiol-functionalization were achieved for all of the hybrid materials, while retaining a regular three-dimensionally ordered macroporous structure. Evidence for bonding of the thiol functional groups to the metal oxide supports was provided by the IR spectra of the materials. Attachment of the functional groups to the metal oxide structures was monitored by shifts in the positions of the characteristic Si–O and S–O bond absorptions upon linking. For example, the propyl–sulfonate precursor (MPSA) exhibited S–O absorptions at 1221, 1198, 1168, and 1065 cm^{-1}. The S–O absorptions for the respective products were observed at 1223, 1149, and 1047 cm^{-1} (sample **T3**), and 1241, 1147, and 1044 cm^{-1} (sample **Z3**), Fig. 5. The shift in the positions of these absorptions from the precursors to the products indicates that attachment of the functional groups to the metal oxide has likely occurred. Evidence for attachment of the functional groups to the metal oxides is also supported by the similarity of the absorption positions for each class of thiol group linked to either titania or zirconia. The S–O absorptions for the products with sulfonate linkages are also very similar to the literature values of 1248, 1142, and 1044 cm^{-1} reported for S–O bond vibrations

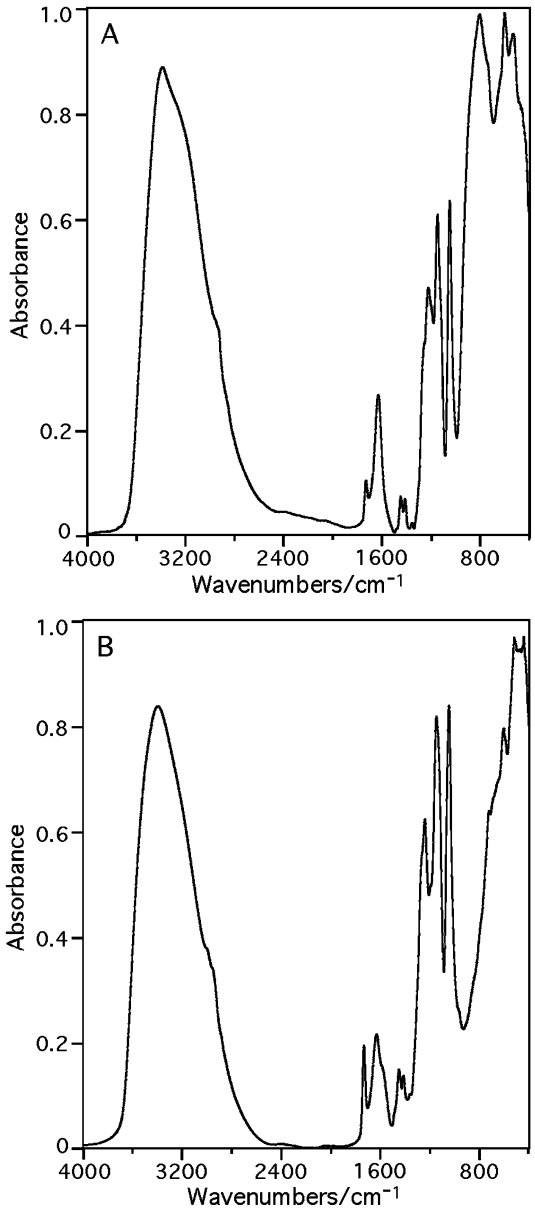

Fig. 5 IR spectra of samples **T3** (A) and **Z3** (B).

of sulfated zirconia,[46] further confirming that linking has occurred. Similar results were obtained for the other samples, and these and other characterization results are given in Table 1.

The thiol–titania and thiol–zirconia macroporous materials with siloxane linkages (samples **T1** and **Z1**, respectively) were characterized by solid state ^{1}H–^{29}Si CP MAS NMR. A broad feature was observed in the spectrum of both samples corresponding to T^3 and T^2 bonding environments, where T^n represents a silicon atom bonded to one organic (R) group and a varying number of O–M (M = Si, Ti, or Zr) and O–H groups, *i.e.* $Si(R)(OM)_n(OH)_{3-n}$. The approximate chemical shifts of these poorly resolved peaks, based on deconvolution, are −68 and −58 ppm for **T1**, and −67 and −57 ppm for **Z1**. For comparison, literature values of T^3 and T^2 peaks for thiol–silica materials with siloxane linkages range from −64 to −72 and −55 to −63 ppm, respectively.[3,7,9–13,15] The presence of Si–O–Ti and Si–O–Zr bonds (from condensation of the siloxane with the metal oxide) would be expected to give a small shift in the peak positions compared to Si–O–Si bonds (from self-condensation of the siloxane), due to the differences in electron densities of Ti and Zr compared to Si. However, the limited resolution of the signals does not allow the identification of the

Table 1 Physical characterization of the hybrid macroporous materials and precursors

Material	IR (S–O) or (Si–O)/cm^{-1}	Pore size/nm	Template size/nm	Surface area/m^2 g^{-1}	Thiol density/ mmol g^{-1}
$(MeO)_3Si$-Pr-SH gel	1119, 1039	—	—	—	—
T1, TiO_2-O_3Si-Pr-SH	1141, 1040	265	300	37	2.24
Z1, ZrO_2-O_3Si-Pr-SH	1125, 1037	415	480	18	1.38
NaO_3S-Et-SH	1206, 1168, 1139, 1058	—	—	—	—
T2, TiO_2-O_3S-Et-SH	1232, 1155, 1047	270	300	12	1.78
Z2, ZrO_2-O_3S-Et-SH	1243, 1151, 1047	450	480	20	1.29
NaO_3S-Pr-SH	1221, 1198, 1168, 1065	—	—	—	—
T3, TiO_2-O_3S-Pr-SH	1223, 1149, 1047	275	300	12	1.71
Z3, ZrO_2-O_3S-Pr-SH	1241, 1147, 1044	460	480	14	1.35

Table 2 Metal ion adsorption data for the hybrid macroporous materials

Material	M/SH (M = Ti,Zr) mol/mol	Hg(II) adsorbed/ mmol g^{-1}	Pb(II) adsorbed/ mmol g^{-1}	Adsorption efficiency mol/mol	
				Hg/SH	Pb/SH
T1, TiO_2-O_3Si-Pr-SH	2.61	0.43	0.47	0.19	0.21
T2, TiO_2-O_3S-Et-SH	3.28	0.33	0.82	0.19	0.46
T3, TiO_2-O_3S-Pr-SH	3.63	1.41	1.24	0.82	0.72
Z1, ZrO_2-O_3Si-Pr-SH	3.41	0.54	0.36	0.39	0.26
Z2, ZrO_2-O_3S-Et-SH	3.52	0.45	0.27	0.35	0.21
Z3, ZrO_2-O_3S-Pr-SH	3.66	0.87	0.36	0.64	0.27

specific bonding mode. It is likely that a mixture of Si–O–Si and Si–O–Ti (or Zr) bonds are present.

Heavy metal ion adsorption

The ability of the hybrid macroporous materials to remove the heavy metal ions mercury(II) and lead(II) from solution was tested by stirring the adsorbents in aqueous solutions of the metal ions. Results of the metal ion adsorption tests are summarized in Table 2. The adsorption capacity of the hybrid macroporous materials for mercury(II) ions ranged from 0.33–1.41 mmol of Hg(II) ions adsorbed per gram of adsorbent. The Hg(II) loading was similar for each class of functional group, with the best results obtained for the thiol–metal oxides with propyl–sulfonate linkages. The adsorption efficiencies ranged from 0.19–0.82 mol of Hg(II) ions adsorbed per mol of thiol groups in the adsorbents. Less than stoichiometric adsorption is most likely due to a limited accessibility of the thiol groups in the interior of the walls. The adsorption capacity for lead(II) ions ranged from 0.27–1.24 mmol g^{-1}, with the thiol–titania samples containing sulfonate linkages exhibiting the highest loadings. The adsorption efficiencies for Pb(II) ions ranged from 0.21–0.72 mol of Pb(II) ions adsorbed per mol of thiol groups. The heavy metal ion loading capacities achieved with the hybrid macroporous titania and zirconia adsorbents are competitive with results of *ca.* 0.10–3.00 mmol g^{-1} for Hg(II) and 0–0.35 mmol g^{-1} for Pb(II) obtained for various porous silica-based adsorbents.[3–15]

Regeneration of adsorbents

To test the reusability of the hybrid macroporous adsorbents, the Hg(II) ion loaded samples were treated with 1 M hydrochloric acid to remove the heavy metal ions. The leached materials were then subjected to a second round of metal ion adsorption testing. The results for metal ion adsorption using the regenerated adsorbents are summarized in Table 3. All of the hybrid macroporous materials maintained greater than 50% of the original metal ion loading capacity. The regenerated thiol–zirconia samples generally retained higher loading capacities than the thiol–titania samples, giving average capacities of 74% and 58% of the original loading, respectively.

Table 3 Metal ion adsorption data for the regenerated hybrid macroporous materials

Material	Hg(II) adsorbed/mmol g^{-1}		% Original metal ion loading capacity
	Initial test	2nd test	
T1, TiO_2-O_3Si-Pr-SH	0.43	0.27	63
T2, TiO_2-O_3S-Et-SH	0.33	0.19	58
T3, TiO_2-O_3S-Pr-SH	1.41	0.75	53
Z1, ZrO_2-O_3Si-Pr-SH	0.54	0.37	69
Z2, ZrO_2-O_3S-Et-SH	0.45	0.34	76
Z3, ZrO_2-O_3S-Pr-SH	0.87	0.67	77

Conclusions

Several methods have been presented for the preparation of a new class of heavy metal ion adsorbents, composed of thiol functional groups attached to a macroporous titania or zirconia matrix. The synthetic flexibility of the colloidal crystal templating approach allowed the preparation of the porous materials *via* direct synthesis procedures, therefore providing a means to incorporate high levels of thiol groups into the materials. The choice of titania and zirconia frameworks allowed multiple bonding modes to be explored, as demonstrated by the siloxane and sulfonate bonding modes presented here. The hybrid macroporous materials functioned as toxic metal ion adsorbents, removing mercury and lead ions from solution. The hybrid macroporous adsorbents could be recycled by leaching the loaded metal ions from the materials by an acid wash and using the regenerated samples for further metal ion adsorption. The improved mass transport offered by materials with macroporous structures makes the hybrid materials reported here potential adsorbents for cleanup of wastewater using flow systems.

Acknowledgements

We thank the U.S. Army Research Laboratory and the U.S. Army Research Office under contract/grant number DAAD 19-01-1-0512, the National Science Foundation (DMR-9701507), the MRSEC program of the NSF (DMR-9809364), and the David and Lucile Packard Foundation for support of this research. M.C.C. thanks the PFI Program and PB98-0673-C02-02 Project of MCYT (Spain) for financial support, and the

hospitality of the Stein group during her stay at the University of Minnesota.

References

1 A. K. SenGupta, *Environmental separation of heavy metals*, CRC Press, New York, 2002.
2 M. Volkan, O. Y. Ataman and A. G. Howard, *Analyst*, 1987, **112**, 1409–1412.
3 E. F. S. Vieira, J. d. A. Simoni and C. Airoldi, *J. Mater. Chem.*, 1997, **7**, 2249.
4 L. Mercier and C. Detellier, *Environ. Sci. Technol.*, 1995, **29**, 1318–1323.
5 A. Stein, B. J. Melde and R. C. Schroden, *Adv. Mater.*, 2000, **12**, 1403–1419 and references therein.
6 X. Feng, G. E. Fryxell, L.-Q. Wang, A. Y. Kim, J. Liu and K. M. Kemner, *Science*, 1997, **276**, 923–926.
7 L. Mercier and T. J. Pinnavaia, *Adv. Mater.*, 1997, **9**, 500–503.
8 J. Liu, X. Feng, G. E. Fryxell, L.-Q. Wang, A. Y. Kim and M. Gong, *Adv. Mater.*, 1998, **10**, 161–165.
9 M. H. Lim, C. F. Blanford and A. Stein, *Chem. Mater.*, 1998, **10**, 467–470.
10 L. Mercier and T. J. Pinnavaia, *Environ. Sci. Technol.*, 1998, **32**, 2749–2754.
11 A. M. Liu, K. Hidajat, S. Kawi and D. Y. Zhao, *Chem. Commun.*, 2000, 1145–1146.
12 R. I. Nooney, M. Kalyanaraman, G. Kennedy and E. J. Maginn, *Langmuir*, 2001, **17**, 528–533.
13 Y. Mori and T. J. Pinnavaia, *Chem. Mater.*, 2001, **13**, 2173–2178.
14 A. Bibby and L. Mercier, *Chem. Mater.*, 2002, **14**, 1591–1597.
15 J. Brown, L. Mercier and T. J. Pinnavaia, *Chem. Commun.*, 1999, 69–70.
16 T. Yanagisawa, T. Shimizu, K. Kuroda and C. Kato, *Bull. Chem. Soc. Jpn.*, 1990, **63**, 988–992.
17 C. T. Kresge, M. E. Leonowicz, W. J. Roth, J. C. Vartuli and J. S. Beck, *Nature*, 1992, **359**, 710–712.
18 J. S. Beck, J. C. Vartuli, W. J. Roth, M. E. Leonowicz, C. T. Kresge, K. D. Schmitt, C. T.-W. Chu, D. H. Olson, E. W. Sheppard, S. B. McCullen, J. B. Higgins and J. L. Schlenker, *J. Am. Chem. Soc.*, 1992, **114**, 10834–10843.
19 S. Inagaki, Y. Fukushima and K. Kuroda, *J. Chem. Soc., Chem. Commun.*, 1993, 680–682.
20 A. Stein, *Microporous Mesoporous Mater.*, 2001, **44–45**, 227–239 and references therein.
21 O. D. Velev, T. A. Jede, R. F. Lobo and A. M. Lenhoff, *Nature*, 1997, **389**, 447–448.
22 B. T. Holland, C. F. Blanford and A. Stein, *Science*, 1998, **281**, 538–540.
23 J. E. G. J. Wijnhoven and W. L. Vos, *Science*, 1998, **281**, 802–804.
24 O. D. Velev, P. M. Tessier, A. M. Lenhoff and E. W. Kaler, *Nature*, 1999, **401**, 548.
25 H. Yan, C. F. Blanford, B. T. Holland, M. Parent, W. H. Smyrl and A. Stein, *Adv. Mater.*, 1999, **11**, 1003–1006.
26 P. Jiang, J. Cizeron, J. F. Bertone and V. L. Colvin, *J. Am. Chem. Soc.*, 1999, **121**, 7957–7958.
27 P. V. Braun and P. Wiltzius, *Nature*, 1999, **402**, 603–604.
28 A. Blanco, E. Chomski, S. Grabtchak, M. Ibisate, S. John, S. W. Leonard, C. Lopez, F. Meseguer, H. Miguez, J. P. Mondia, G. A. Ozin, O. Toader and H. M. van Driel, *Nature*, 2000, **405**, 437–440.
29 Y. A. Vlasov, X.-Z. Bo, J. C. Sturm and D. J. Norris, *Nature*, 2001, **414**, 289–293.
30 S. H. Park and Y. Xia, *Chem. Mater.*, 1998, **10**, 1745–1747.
31 P. Jiang, K. S. Hwang, D. M. Mittleman, J. F. Bertone and V. L. Colvin, *J. Am. Chem. Soc.*, 1999, **121**, 11630–11637.
32 A. A. Zakhidov, R. H. Baughman, Z. Iqbal, C. Cui, I. Khayrullin, S. O. Dantas, J. Marti and V. G. Ralchenko, *Science*, 1998, **282**, 897–901.
33 B. T. Holland, C. F. Blanford, T. Do and A. Stein, *Chem. Mater.*, 1999, **11**, 795–805.
34 B. J. S. Johnson and A. Stein, *Inorg. Chem.*, 2001, **40**, 801–808.
35 R. C. Schroden, C. F. Blanford, B. J. Melde, B. J. S. Johnson and A. Stein, *Chem. Mater.*, 2001, **13**, 1074–1081.
36 U. A. El-Nafaty and R. Mann, *Chem. Eng. Sci.*, 1999, **54**, 3475–3484.
37 H. Yan, K. Zhang, C. F. Blanford, L. F. Francis and A. Stein, *Chem. Mater.*, 2001, **13**, 1374–1382.
38 B. Lebeau, C. E. Fowler, S. Mann, C. Farcet, B. Charleux and C. Sanchez, *J. Mater. Chem.*, 2000, **10**, 2105–2108.
39 P. Judeinstein and C. Sanchez, *J. Mater. Chem.*, 1996, **6**, 511–525 and references therein.
40 J. G. C. Shen, T. H. Kalantar, R. G. Herman, J. E. Roberts and K. Klier, *Chem. Mater.*, 2001, **13**, 4479–4485 and references therein.
41 P. H. Mutin, C. Delenne, D. Medoukali, R. Corriu and A. Vioux, *Mater. Res. Soc. Symp. Proc.*, 1998, **519**, 345–350.
42 G. Guerrero, P. H. Mutin and A. Vioux, *Chem. Mater.*, 2000, **12**, 1268–1272.
43 G. Guerrero, P. H. Mutin and A. Vioux, *Chem. Mater.*, 2001, **13**, 4367–4373.
44 J. W. Goodwin, R. H. Ottewill, R. Pelton, G. Vianello and D. E. Yates, *Br. Polym. J.*, 1978, **10**, 173–180.
45 D. Zou, S. Ma, R. Guan, M. Park, L. Sun, J. J. Aklonis and R. Salovey, *J. Polym. Sci., Part A: Polym. Chem.*, 1992, **30**, 137–144.
46 A. A. M. Ali and M. I. Zaki, *Thermochim. Acta*, 1999, **336**, 17–25.